Journal of Statistical Physics, Vol. 52, Nos. 5/6, 1988

Quantum Monte Carlo Study of a Proton in an Electron Gas

G. Sugiyama[1], L. Terray[1], and B. J. Alder[1]

Received April 22, 1988

The polarization of jellium by a fixed proton impurity at 0 K is determined for an electron density range from metallic to dilute using the quantum Monte Carlo algorithm. Preliminary results show the correct H^- binding limit for the impurity in a dilute electron gas. The screening indicates transitions from two- to one-electron binding and from localized to delocalized electrons as the jellium density increases. The results are compared to density functional calculations. Pair distribution functions, Friedel oscillations, and binding energies are discussed.

KEY WORDS: Jellium; proton impurity; Friedel oscillations; quantum Monte Carlo.

1. INTRODUCTION

The addition of a proton (H atom) to a host electronic system is the simplest example of an impurity in a metal. At low electronic density, the H atom is expected to attract a second electron, forming a H^- system. As the density increases, the second electron is no longer bound and the impurity acts as a neutral H atom weakly polarizing the medium. At metallic densities, the H atom dissociates into a proton and an electron. Nonlinear screening occurs in the system, since the metallic electrons are strongly perturbed by their interaction with the bare Coulomb potential of the proton. In this study, the quantum Monte Carlo algorithm has been used to investigate the effects of a proton in jellium—an electron gas model for the metal with a charge-neutralizing uniform positive background.

The impurity-in-jellium model has been studied using density functional theory.[1] This method has had various degrees of success in

[1] Lawrence Livermore National Laboratory, Livermore, California 94550.

0022-4715/88/0900-1221$06.00/0

applications to a number of atomic, molecular, and solid state problems. The density functional approach reduces the quantum many-body problem to a single-particle Schrödinger equation. Energies generated by this method are therefore one-particle eigenvalues which do not have an exact physical interpretation as spectral values or system energies. The method yields only self-consistent solutions to the system of interest, instead of strict bounds on the energies. Further, actual calculations using this approach involve the local density approximation (LDA) or a first-order gradient correction to the LDA, resulting in an approximate effective exchange-correlation potential which is valid only for slowly varying electronic densities.[2]

Two different density functional approaches to the impurity problem have been used, the standard Hohenberg–Kohn–Sham method[3–5] and a qualitative technique involving quasiatoms.[6] The quasiatom method treats the impurity and electronic screening cloud as a unit. It uses the uniform density approximation, a variant of the LDA, and gives estimates of the change in energy caused by the addition of an impurity. It is unclear whether the LDA is valid for the proton-in-metal problem, where electron densities are large and rapidly varying near the proton. Density functional self-consistency is difficult to achieve for the system, due to strong perturbations in the electronic charge caused by the bare Coulomb force. The method fails in applications to atomic systems, such as the H atom, due to improper cancellation of the self-energy term with the appropriate piece of the approximate exchange-correlation potential, leading to instability of negative ions in the LDA.[7]

Due to the limitations of density functional methods and especially of the LDA approximation, a study of the impurity problem using a first-principles solution of the Schrödinger equation is of interest. The quantum Monte Carlo algorithm[8] solves the many-body problem exactly within statistical error bars, including all of the correlation energy, rather than approximately by reduction to a set of one-particle equations. The method has successfully resolved questions on properties and phase transitions in a variety of systems, including the electron gas (Wigner crystallization),[9] liquid and solid helium,[10] chemical molecules,[11] bulk and molecular hydrogen,[12] and metallic lithium.[13]

2. QUANTUM MONTE CARLO ALGORITHM

The quantum Monte Carlo algorithm involves several stages of progressively greater accuracy: variational, fixed-node diffusion, and Green's function simulations, and the released node Green's function method. The first three yield strict upper bounds to the ground-state

energy, while the released node method provides exact answers within statistics. In this preliminary study, the variational and fixed-node algorithms were used to study the screening effects of a proton in jellium. A summary of the algorithm follows, along with a description of the treatment of the proton impurity system.

Variationally, the total energy of a system with Hamiltonian $\mathbf{H}$ is given by the minimum with respect to the set of all possible trial functions Ψ_T of the expectation value,

$$E = \underset{[\Psi_T]}{\text{Min}} \frac{\int \Psi_T \mathbf{H} \Psi_T}{\int |\Psi_T|^2} \tag{1}$$

In practice, a limited subset of trial functions are selected and minimized with respect to a number of parameters. The result is an upper bound on the energy that is dependent upon the nature of the trial wave function. In the variational phase of the quantum Monte Carlo method, the wave function is described by an ensemble of configurations each consisting of a set of particle coordinates. The Metropolis Monte Carlo algorithm is then used to sample the coordinate configurations and evaluate expectation values for the quantities of interest.[14] This phase of the calculation selects good trial functions and provides initial configurations for the diffusion or Green's function simulations which follow. The form of the trial function is discussed below.

The diffusion Monte Carlo algorithm computes a more accurate solution of the Schrödinger equation.[11] The Schrödinger equation in imaginary time is treated as a diffusion equation. The many-body wave function Ψ satisfies

$$\mathbf{H}\Psi(\mathbf{R}, t) = \left[-\sum_{i=1}^{N} \frac{\hbar^2}{2m} \nabla_i^2 + V(\mathbf{R}) - E_T \right] \Psi(\mathbf{R}, t) \tag{2}$$

where $\mathbf{R} = (\mathbf{r}_1, \mathbf{r}_2, ..., \mathbf{r}_N)$ is the $3N$-dimensional vector of the electronic coordinates $\mathbf{r}_i$, t is the imaginary time, and

$$V(\mathbf{R}) = \sum_{i<j}^{N} \frac{e^2}{r_{ij}} - \sum_{i}^{N} \frac{Z_\alpha e^2}{r_{i\alpha}} \tag{3}$$

is the potential energy of the impurity and jellium, using standard Coulomb interactions. The sums run over the electronic coordinates i, j with $r_{ij} \equiv |\mathbf{r}_i - \mathbf{r}_j|$ and $r_{i\alpha} \equiv |\mathbf{r}_i - \mathbf{r}_\alpha|$, where $\mathbf{r}_\alpha$ is the location of the impurity. E_T is a constant trial energy, which is subtracted from the potential energy for computational convenience. The kinetic term in the Schrödinger equation (2) is stochastically represented as standard diffusion with

diffusion constant $\hbar^2/2m$. The potential and trial energy terms act as branching, generating a birth-and-death process. The solution converges exponentially to the ground state.

The many-body wave function Ψ can be interpreted as the density of diffusing particles as long as it is everywhere of one sign. This is clearly not the case for fermions, where the many-body wave function possesses nodal surfaces in $3N$ space [defined by $\Psi(\mathbf{R}) = 0$]. However, this difficulty can be overcome by introducing a trial wave function Ψ_T whose nodes act as absorbing barriers to the diffusion process. This fixed-node method constrains the many-body wave function to have the approximate nodal surface of Ψ_T, leading to an upper-bound criterion on the ground-state energy. In principle, the nodal surfaces could be varied to obtain the best upper bound on the energy, although in practice it is difficult to parametrize Ψ_T in a systematic fashion. For the electron gas, the dependence upon the location of the nodes of the trial wave function has been shown to be weak.[9] However, for an accurate upper bound, Ψ_T should be chosen as close to the true ground-state wave function as is feasible. The released-node Green's function algorithm eliminates the constraint on the trial function nodal surface to obtain the true ground-state energy of the system.

The stochastic solution of the diffusion equation is performed on an initial ensemble of several hundred configurations of particle coordinates generated by the variational Monte Carlo run. For solids, a finite simulation box or supercell with periodic boundary conditions is used. The long-range Coulomb interaction energies are evaluated by Ewald summation.

The quantum Monte Carlo method yields results whose accuracy is determined statistically within the simulation. The algorithm in principle works for all two-body potentials, crystal phases, and elements. The method has so far been practical only for the light elements due to the required computer time. The limitations of the algorithm involve the finite size of the simulation box, difficulties in determining small energy differences, the upper-bound approximation of the fixed-node method for treating fermion statistics, and the transient nature of the released-node Green's function step.

Trial wave function. The standard form for the trial wave function Ψ_T that has been successful in previous studies consists of the product of a Slater determinant of single-particle orbitals multiplied by a pair-product Jastrow factor **J**:

$$\Psi_T = \det |\Phi_{ij}^{+}| \det |\Phi_{ij}^{-}| \mathbf{J} \tag{4}$$

where Φ_{ij} are the one-particle wave functions in the Slater determinant, with the superscripts plus and minus denoting the two possible spin states. The determinants provide the required fermion antisymmetry. The Jastrow factor incorporates two-body correlation effects

$$\mathbf{J} = \exp\left(- \sum_{i,j}^{N} u_{ij} - \sum_{i}^{N} u_{i\alpha} \right) \tag{5}$$

and involves a sum of the electron–impurity, $u_{i\alpha}$, and the electron–electron, u_{ij}, pair correlation terms. These terms exactly satisfy the cusp conditions: the singularities of the wave function for zero pair separation due to the Coulombic divergence of the potential. The random phase approximation (RPA)[14] is typically used for the long-range behavior of the Jastrow terms.

In this study, all the densities investigated were below the Wigner crystallization regime, so plane waves were employed as the Slater determinant states of the trial function for the background jellium. The number of jellium electrons per simulation box was selected to obtain a closed shell structure for the plane wave states, in order to reduce the number dependence of the simulations. Electrons localized about the impurity were treated as Gaussians with parametrized widths. Such simple forms have been adequate in previous applications to the electron gas,[9] metallic hydrogen,[12] and lithium.[13]

The variational algorithm evaluates the trial wave function energy. In this step, the electrons are forced into localized or delocalized states, depending on the choice of Slater determinant states. In contrast, the diffusion results are limited only by the fixed-node approximation and allow the electrons to localize or delocalize in order to minimize the energy.

3. RESULTS

The Schrödinger equation for a jellium system with a proton impurity was solved using the variational and fixed-node diffusion algorithms. For a given electron gas density, systems with jellium electrons in plane wave states and no proton, a proton and an added localized electron, a proton and and an added delocalized electron, and a proton and two localized electrons were simulated. The additional electrons were added in order to maintain the same jellium density at large distances from the impurity proton. For the case of two added electrons, a correction for the periodic images was implemented in order to compensate for the net charge of the system.

Calculations were performed on a cubic supercell simulation box with periodic boundary conditions, the impurity being located at a fixed

position. The impurity was present as one copy per periodic cell, so corrections based on the finite simulation box size must be determined. The boxes must be of sufficient size so that the effects of the impurity are negligible at the box boundaries.

The impurity problem requires considerable numerical accuracy because it involves small energy values which are the differences between large system energies. The energy for the addition of the impurity, which will be called the impurity energy, is given by

$$\Delta E^{\mathrm{H}} = E_{N+\mathrm{H}} - E_N \tag{6a}$$

and

$$\Delta E^{\mathrm{H}^-} = E_{N+\mathrm{H}^-} - E_N \tag{6b}$$

where $E_{N+\mathrm{H}}$ and $E_{N+\mathrm{H}^-}$ are the energies of the systems with N jellium electrons, an impurity proton, and either one or two additional electrons, respectively. In density functional theory, the impurity energy is

$$\Delta E_{\mathrm{dft}} = E_{N+1}[n(\mathbf{r})] - E_N[n(\mathbf{r})] \tag{6c}$$

where E_{N+1} is the energy of a system with an impurity of charge 1 and $N+1$ electrons and E_N is the energy of the jellium system with N electrons, both of which are functionals of the electron density $n(\mathbf{r})$. In density functional calculations performed so far, it has not been possible to directly determine the difference between the H and H^- state of the impurity.

Quantum Monte Carlo calculations of the proton in jellium were performed over a density range from $r_s = 1.0$ to $r_s = 25.0$ for systems of 54-electron jellium, 54-electron jellium with a proton and an additional delocalized electron, 54-electron jellium with a proton and one localized electron, and 54-electron jellium with a proton and two localized electrons. At low densities ($r_s > 100$), the jellium system forms a Wigner lattice[9] and the added H atom would be expected to combine at some lattice site with an electron to form an H^-. An isolated H^- atom has a binding energy -1.05 Ryd. At low fluid densities, the quantum Monte Carlo results show that the H^- is the preferred ground state of the impurity (the system of lowest energy at that density) with $\Delta E^{\mathrm{H}^-} = -1.04$ Ryd at $r_s = 25$. Density functional theory fails in the low-density limit, as discussed earlier.

Preliminary variational results are shown in Fig. 1, which plots the total system energies versus density for medium to metallic r_s. There is a minimum in the system energy at $r_s \approx 4.0$. For low densities ($r_s > 7$) the ground state favors two localized electrons, while at metallic densities ($r_s < 3$) delocalized electrons are preferred. Although difficult to see on the scale of the plot, the calculations show changes in the preferred ground-

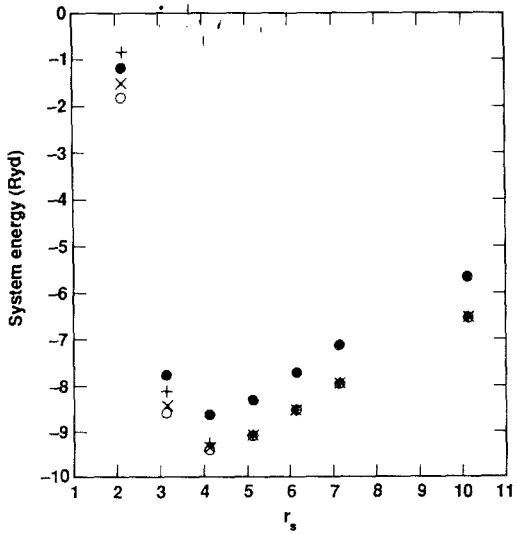

Fig. 1. System energy versus density in units of r_s for (●) the electron gas, (○) the electron gas plus an impurity proton and delocalized electron, (×) the electron gas plus an impurity proton and a localized electron, and (+) the electron gas plus an impurity proton and two localized electrons. The energies are in Rydbergs.

state system in the density range $4 < r_s < 6$ from two to one to no bound electrons. Further runs are required to determine the exact transition points.

Table I lists the impurity energies ΔE^H and ΔE^{H^-} from quantum Monte Carlo and ΔE_{dft} from density functional calculations [Eqs. (6)]. Figure 2 plots the quantum Monte Carlo values, showing a crossing of the curves for two- and one-electron localization at $5 < r_s < 6$. The density functional method does not allow a direct determination of the nature of electronic binding to the impurity. However, a negative slope of the impurity energy ΔE_{dft} as a function of density syggests an overscreening of the impurity and may be interpreted as a precursor to a negative ion. Results from density functional calculations[1] give a negative slope for values greater than $r_s = 4.6$, which agrees approximately with the crossing of the curves for the H and H^- systems obtained by quantum Monte Carlo. The density functional quasiation slope theorem[6] implies that a minimum in the impurity energy curve ΔE_{dft} versus density should occur at the density where the mean potential vanishes. Neither our calculations nor standard density functional calculations[3,4] show this minimum (Table I).

Also listed in Table I are the density functional binding energies of the system defined as $E_b = 2\varepsilon_b$, where ε_b is the one-electron eigenvalue of the system. Significant changes in this energy occur when gradient corrections

Table I. Impurity Energies for the Electron Gas System[a]

r_s	ΔE_v^H	$\Delta E_v^{H^-}$	ΔE_d^H	$\Delta E_d^{H^-}$	ΔE_{dft} [4]	ΔE_{dft} [3]	E_b [3]
1.0	—	—	—	—	0.968	0.938	—
2.0	−0.38 (2)	0.35 (2)	−0.60 (1)	−0.05 (1)	−0.854	−0.876	−0.00052
3.0	−0.67 (2)	−0.38 (2)	—	—	—	−1.062	−0.0272
4.0	−0.72 (1)	−0.64 (2)	—	—	−1.086	−1.096	−0.0428
5.0	−0.78 (2)	−0.73 (2)	—	—	—	−1.098	−0.0462
6.0	−0.77 (1)	−0.80 (2)	—	—	—	−1.096	−0.0482
7.0	−0.81 (2)	−0.82 (2)	—	—	—	—	—
10.0	−0.84 (1)	−0.87 (1)	—	—	—	—	—
15.0	−0.96 (2)	−0.97 (2)	—	—	—	—	—
25.0	−0.97 (2)	−1.04 (2)	—	—	—	—	—

[a] Energies are in Rydbergs, densities in $r_s = r_0/a_0$, where a_0 is the Bohr radius and r_0 is defined in terms of the number density of the electrons $n = 1/(4\pi r_0^3/3)$. The quantum Monte Carlo variational (ΔE_v^H and $\Delta E_v^{H^-}$) and diffusion (ΔE_d^H and $\Delta E_d^{H^-}$) impurity energies and the density functional impurity energies (ΔE_{dft}) from two different calculations[3,4] are defined in Eq. (6) in the text. E_b is the density functional binding energy.[3]

are utilized. The interpretation of the one-electron eigenvalues as physical quantities is unproven and calculations have shown that these states are too shallow to be interpretable as true bound states.[5] Quantum Monte Carlo estimates of the binding energy of the impurity, from the energy difference of the system with a proton impurity and a localized electron and a

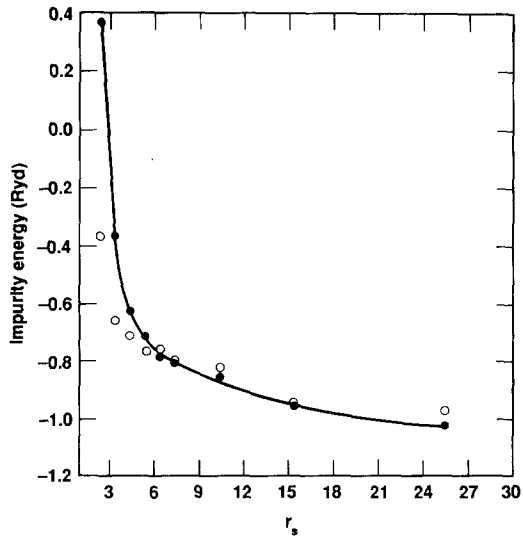

Fig. 2. Impurity energy versus density in units of r_s for the (●) H^- and (○) H systems. The line is a spline fit for the H^- system.

system with a proton impurity and a delocalized electron, are on the order of 10^{-2} Ryd. This difference is related to the energy required to promote an electron from a bound to an unbound state. Better estimates should be obtained when more simulations have been performed.

The variational pair distribution functions are shown in Fig. 3–5. Figure 3 shows the electron–electron correlation function $g_{e^-e^-}(r)$ for the jellium system (54 electrons) for $r_s = 4$. It exhibits the standard behavior for a uniform electron gas—a constant density except for the Pauli principle repulsion at $r = 0$. The electron–proton pair distribution functions $g_{e^-p}(r)$ for the ground-state system at the densities $r_s = 4$, 6, and 10 are plotted in Fig. 4. As expected, the electron density centered on the proton impurity increases as the density of the electron gas decreases. An enlarged plot of the function in Fig. 5 shows oscillations about the uniform electron gas background. The amplitude of the oscillations increase with decreasing density. Since the pair distribution function $g_{e^-p}(r)$ is defined as the probability of finding an electron at a distance r from the impurity, the oscillation nodal structure is directly related to the Friedel oscillations in the number density.

Friedel oscillations[15] have the functional form

$$\delta n(r) = A \cos(2k_F r + \phi)/r^3 \tag{7}$$

where $\delta n(r)$ is the excess charge density, ϕ is a phase shift determining the first node, k_F is the Fermi wave vector, and A is an amplitude normalizing

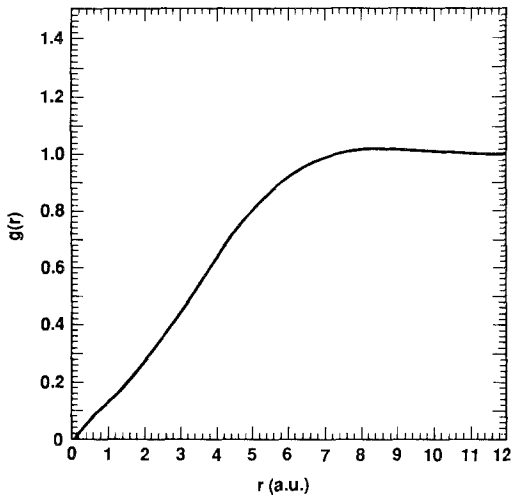

Fig. 3. Electron–electron pair distribution function $g_{e^-e^-}(r)$ for $r_s = 4$ for the electron gas (54 electrons).

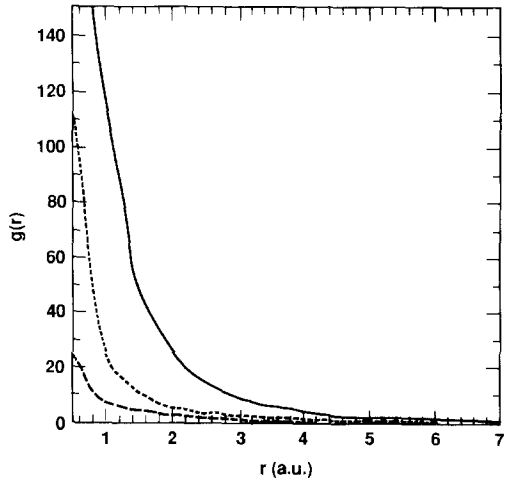

Fig. 4. Electron–proton pair distribution function $g_{e^-p}(r)$ for the ground-state systems at densities (- -) $r_s = 4$, ($\cdots$) 6, and (—) 10.

the function to 1.0 for a uniform electron gas. Table II shows the first node $r_{\text{dft}}^{\text{node}}$ of the displaced density for Friedel oscillations from a density functional calculation[4] and the half-period $\delta r^{\text{node}} = \pi/2k_{\text{F}}$ [Eq. (7)]. Quantum Monte Carlo values are also given for the first node r_v^{node} and the half-period δr_v^{node} of the pair distribution $g_{e^-p}(r)$ oscillations. The period of the pair distribution oscillations is on the same order as the Friedel period.

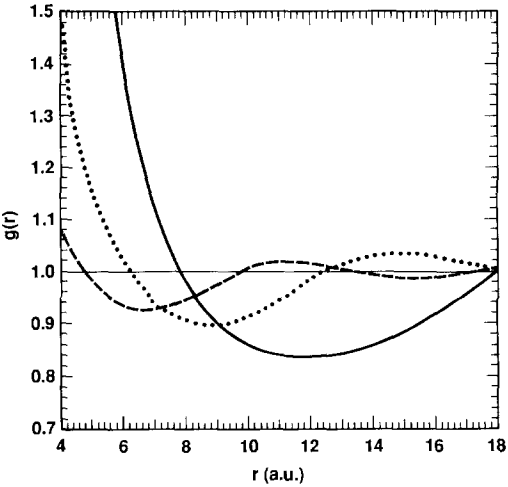

Fig. 5. Electron–proton pair distribution function $g_{e^-p}(r)$ for the ground-state systems at densities (- -) $r_s = 4$, ($\cdots$) 6, and (—) 10, showing the Friedel oscillations.

Table II. First Node $r_{\text{dft}}^{\text{node}}$ [4] and Half-Period $\delta r^{\text{node}} = 1/k_F$ of the Displaced Density for Friedel Oscillations $\delta n(r) = A\cos(2k_F r)\phi)/r^3$ Compared with First Node r_v^{node} and Half-Period δr_v^{node} of Pair Distribution Oscillations from Quantum Monte Carlo Calculations[a]

r_s	$\delta r^{\text{node}} = (\pi^2/18)^{1/3} r_s$	$r_{\text{dft}}^{\text{node}}$	δr_v^{node}	r_v^{node}
1.0	0.8185	2.88	—	—
2.0	1.6370	2.37	—	—
3.0	2.4555	—	—	—
4.0	3.2739	3.30	4.5	5.
5.0	4.0924	—	—	—
6.0	4.9109	—	6.0	6.
10.0	8.1848	—	10.0	8.

[a] Lengths are in units of a.u.

The r^{node} values are slightly larger than the density functional results. With better statistics it can be determined whether there are significant differences in these quantities.

4. DISCUSSION AND CONCLUSIONS

More diffusion and selected released-node Green's function runs must be performed before the quantum Monte Carlo algorithm can be used to assess the accuracy of the density functional approach. These simulations will generate better statistics and, more importantly, results which are not dependent on the exact form of the trial wave function. Preliminary diffusion calculations indicate that the localized electron system energies are lowered relative to the delocalized system energies, reflecting the convergence of the diffusion simulations to the correct electronic configuration. This will affect the transition points and minima of the energy curves. However, the results are not expected to change qualitatively.

There is a significant energy drop between the variational and diffusion energies, indicating that the trial function is not of an optimal form. The inadequacy of the RPA choice for the Jastrow factor is not surprising, as the strong screening effects due to the proton should significantly affect the two-body correlation terms. The Jastrow factor should be optimized variationally to incorporate more of the pair correlation energies. This will also speed up convergence of the energies.

Dependence of the results on the number of particles in the simulation box must be taken into account by extrapolation to the infinite-number limit, determined from simulations for several supercell sizes at several

densities.[9] The number dependence should depend primarily on the number of nonlocalized electrons. Systems of 54 jellium electrons polarized by a proton impurity will also be studied.

Our preliminary results show that the quantum Monte Carlo algorithm yields physically reasonable results from extreme low density (the correct H^- limit) through the metallic range for the impurity in jellium system. The impurity energy curves can be interpreted to determine a transition from H^- to H-type binding. The pair distribution functions show the correct density-dependent behavior and exhibit Friedel oscillations. Detailed calculations in the transitional density range are underway along with analysis of electron localization, the charge density, and screening around the impurity. We hope to extend the applications of this method to H_2 and positrons in metals.

ACKNOWLEDGMENTS

We thank D. Ceperley for sharing his expertise on quantum Monte Carlo and express our appreciation to the San Diego Supercomputing Center for providing computer time. This work was performed under the auspices of the U.S. Department of Energy Lawrence Livermore National Laboratory contract no. W-7405-ENG-48.

REFERENCES

1. E. Zaremba, in *Density Functional Theory*, J. Keller and J. L. Gazquez, eds. (Springer-Verlag, Berlin, 1983), p. 167, and references cited therein.
2. W. Kohn and L. J. Sham, *Phys. Rev.* **140**:A1133 (1965).
3. E. Zaremba, L. Sander, H. Shore, and J. Rose, *J. Phys. F* **7**:1763 (1977).
4. F. Perrot, *Phys. Rev. A* **25**:489 (1982).
5. P. Jena and K. Singwi, *Phys. Rev. B* **17**:3518 (1978).
6. M. Stott and E. Zaremba, *Phys. Rev. B* **22**:1564 (1980).
7. H. Shore, J. Rose, and E. Zaremba, *Phys. Rev. B* **15**:2858 (1977).
8. D. Ceperley and B. J. Alder, *Science* **231**:555 (1986).
9. D. Ceperley and B. J. Alder, *Phys. Rev. Lett.* **45**:566 (1980).
10. M. H. Kalos, M. A. Lee, and P. A. Whitlock, *Phys. Rev. B* **24**:115 (1981).
11. P. Reynolds, D. Ceperley, B. J. Alder, and W. Lester, *J. Chem. Phys.* **77**:5593 (1982).
12. D. Ceperley and B. J. Alder, *Phys. Rev. B* **36**:2092 (1987).
13. G. Sugiyama, G. Zerah, and B. J. Alder, in *Strongly Coupled Plasmas* (Plenum Press, New York, 1986), p. 229.
14. D. Ceperley, *Phys. Rev. B* **18**:3126 (1978).
15. W. Jones and N. March, *Theoretical Solid State Physics*, Vol. II (Wiley-Interscience, New York, 1973).